Regrown Ohmic Contacts to $In_xGa_{1-x}As$ Approaching the Quantum Conductivity Limit

J. J. M. Law, A. D. Carter, S. Lee, A. C. Gossard, M. J. W. Rodwell
ECE and Materials Departments, University of California, Santa Barbara, CA 93106

We report contact resistances between source-drain regrowth and underlying semiconductor quantum well channels in test structures designed for characterization of source and drain access resistances in III-V MOSFETs. Regrowths included both N+ InAs and N+ graded InAs-$In_xGa_{1-x}As$; channel materials included both unstrained $In_{0.53}Ga_{0.47}As$ and unstrained InAs. The access resistivity correlates strongly with the sheet carrier concentration of the 2-dimensional electron gas, consistent with quantum- but not classical- transport theory. With source-drain regrowth of InAs contacts to InAs channels, the total access resistance is within a factor of two of the inverse of Landauer's quantum-state-limited conductance [1-3]. The state-limited conductance in TLM structures and the ballistic MOSFET transconductance both arise from the same physical process, hence the Landauer term in the TLM resistance does not contribute to the MOSFET source access resistance. Application of TLM data to transistor characterization must therefore correct for the state-limited access resistivity. Samples with contacts regrown onto channels with high $5\cdot10^{14}/cm^2$ sheet carrier concentration, hence low quantum-state-limited resistance, showed extremely low 12.7 Ω–μm access resistivity. This demonstrates the utility of MBE regrowth for source/drain formation in III-V MOS technology.

Epitaxial layer structures (Fig. 1) were prepared by solid source MBE. The channel material for samples (a, b,c,d) were 25 nm of $In_{0.53}Ga_{0.47}As$, 100 nm of n^+ $In_{0.53}Ga_{0.47}As$, 100 nm of n^+ $In_{0.53}Ga_{0.47}As$, and 15 nm InAs. ICP dry etching of SiO_2 formed dummy gates. Samples were oxidized by UV ozone, were dipped in 10:1 H_2O:HC, and were hydrogen cleaned (420 °C , 40 minutes). 60 nm of 5-10×10^{19} cm^{-3} Si-doped regrowth was deposited in the areas not covered by SiO_2. The regrowth was heteroepitaxial n^+ InAs on samples (a) and (b), homoepitaxial n^+ InAs on sample (c), and a non-linear grade from n^+ $In_{0.53}Ga_{0.47}As$ to n^+ InAs on sample (d). After regrowth, a planarization etch process removed regrowth debris from the dummy gate. Samples were metalized with 20 nm Ti / 60 nm Pd / 120 nm Au and mesa-isolated. Contact resistances between the semiconductor regrowth and the channel and contact resistance between the metal and regrowth were extracted by the TLM technique using the four-point technique.

For sample (a) (Table 1), the access resistance was 120 Ω–μm, the channel sheet resistivity 540 Ω, the regrowth sheet resistivity 24 Ω, and the metal/regrowth contact resistivity 2.1 Ω–μm (0.2 Ω–μm^2). For sample (b), the access resistance was 56 Ω–μm, the channel sheet resistivity 32 Ω, the regrowth and channel sheet resistivity 9.2 Ω, and the metal contact resistivity 3.8 Ω–μm (1.5 Ω–μm^2). For sample (c), the access resistance was 68 Ω–μm, the channel sheet resistivity 269 Ω, the regrowth sheet resistivity 19 Ω, and the metal contact resistivity 2.9 Ω–μm (0.4 Ω–μm^2). For sample (d), the access resistance was 12.7 Ω–μm, the channel sheet resistivity 14.5 Ω, the regrowth and channel sheet resistivity 11.3 Ω, and the metal contact resistivity 3.0 Ω–μm (0.8 Ω–μm^2).

Abrupt heterojunctions between the regrowth and channel increase the contact resistivity. This is seen comparing sample (a), InAs regrowth / $In_{0.53}Ga_{0.47}As$ channel, to sample (c), InAs regrowth / InAs channel. It is also seen comparing sample (b), InAs regrowth / $In_{0.53}Ga_{0.47}As$ channel, to sample (d) $In_{0.53}Ga_{0.47}As$-InAs graded regrowth / $In_{0.53}Ga_{0.47}As$ channel. Lower metal-regrowth contact resistivity is observed with more heavily-doped channels. This is seen comparing InAs regrowth on (sample a) thin 25 nm ($n_s=9\cdot10^{12}/cm^2$) versus (sample b) thick 100 nm ($n_s=9\cdot10^{14}/cm^2$) n^+ $In_{0.53}Ga_{0.47}As$ channels. It is also seen comparing (sample b) n^+ InAs regrowth on a thick $In_{0.53}Ga_{0.47}As$ channel with (sample c) n^+ InAs regrowth on a thin InAs channel; despite the InAs/ $In_{0.53}Ga_{0.47}As$ heterointerface in sample (b), lower contact resistivity is observed for the thicker channel.

A TLM structure can show at most Landauer's state-limited conductance; for highly degenerate concentrations, $G_{state}=(q^2 2^{1/2}/\hbar\pi^{3/2})\Sigma_i g_i^{1/2} n_{s,i}^{1/2}$, where g_i is the band degeneracy and $n_{s,i}$ the sheet carrier concentration in the ith vertical eigenstate. The extracted zero-contact-spacing intercept of a TLM measurement is the sum of metal-regrowth and regrowth-channel resistances to the channel and this state-limited resistance $R_{state}=1/G_{state}$. Noting the factor of two associated with the two contacts, the measured 136 Ω-μm resistance (sample c) between two regrown n^+ InAs contacts on the 15 nm InAs channel is within a factor of two of the channel's 80 Ω-μm 2-D state limited resistance. The low 12.4 Ω-μm (11.12 Ω-μm^2) contact-channel access resistivity observed with graded regrowth of contacts to a thick, high n_s channel (sample d) suggests that extremely low contact resistances can be achieved via MBE regrowth. Given that the Landauer resistance observed in a TLM structure will not contribute to MOSFET source access resistance, application of TLM data to transistor characterization in any material system must therefore recognize and correct for the state-limited access resistivity term.

This work was supported by the SRC Non-Classical CMOS Research Program. A portion of this work was performed in the UCSB nanofabrication facility, part of the NSF funded NNIN network

[1] R. Landauer, IBM J. Res. Dev. **1**, 223 (1957).
[2] P. M. Solomon *et al.*, IEDM Tech. Dig., 1989, p. 405.
[3] J. Guo, *et al.*, IEEE Elec. Dev. Lett. **33**, 525 (2012).

978-1-4673-1164-9/12/$31.00 ©2012 IEEE

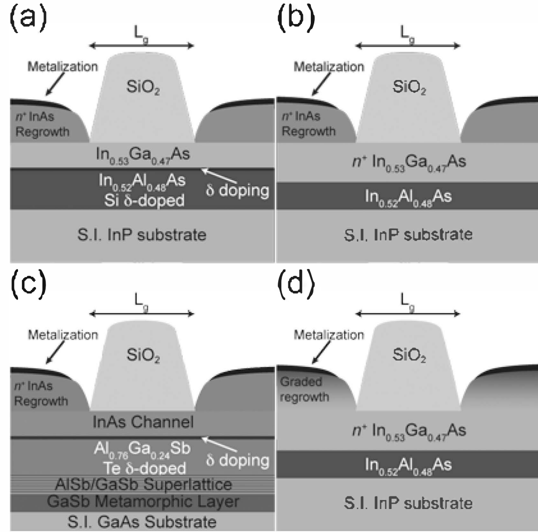

Figure 1: Channel-regrowth contact resistance test structures for (a) the 25 nm $In_{0.53}Ga_{0.47}As$ channel with n^+ InAs regrowth, (b) the 100 nm n^+ $In_{0.53}Ga_{0.47}As$ with n^+ InAs regrowth, (c) 15 nm InAs channel with n^+ InAs regrowth, and (d) 100 nm n^+ $In_{0.53}Ga_{0.47}As$ channel with graded regrowth.

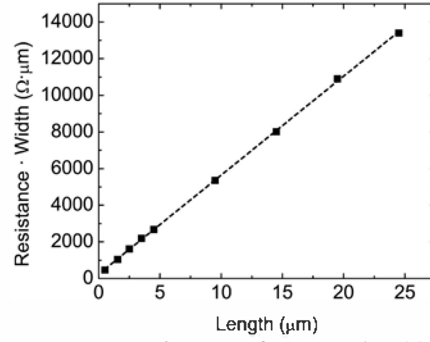

Figure. 2: TLM resistance for sample (a), 25 nm $In_{0.53}Ga_{0.47}As$ channel with n^+ InAs regrowth.

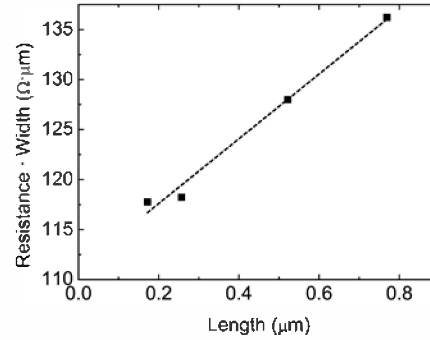

Figure. 3: TLM resistance for sample (b), 100 nm n^+ $In_{0.53}Ga_{0.47}As$ with n^+ InAs regrowth.

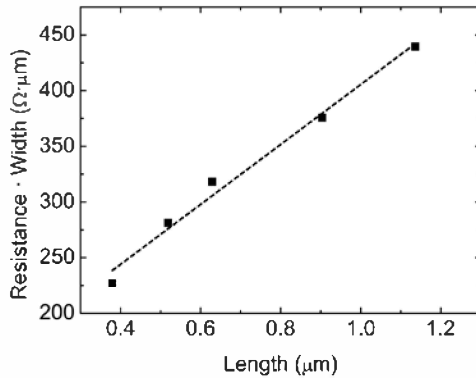

Figure 4: TLM resistance for sample (c), 15 nm InAs channel with n^+ InAs regrowth.

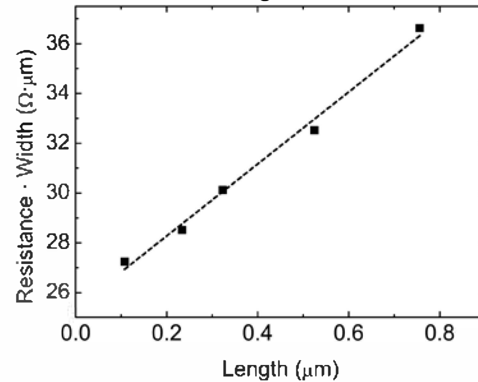

Figure 5: TLM resistance for sample (d), 100 nm n^+ $In_{0.53}Ga_{0.47}As$ channel with graded regrowth.

Table 1: Sample layer structures and measured resistivities.

Sample	(a)	(b)	(c)	(d)
N+ regrowth				
composition	InAs	InAs	InAs	$In_{0.53}Ga_{0.47}As \rightarrow$ InAs
thickness	60 nm	60 nm	60 nm	60 nm
doping	$5\text{-}10\cdot10^{19}/cm^3$	$5\text{-}10\cdot10^{19}/cm^3$	$5\text{-}10\cdot10^{19}/cm^3$	$5\text{-}10\cdot10^{19}/cm^3$
sheet resistivity	23.8 Ω	7.4 Ω	19.3 Ω	11.3 Ω
channel				
composition	$In_{0.53}Ga_{0.47}As$	$In_{0.53}Ga_{0.47}As$	InAs	$In_{0.53}Ga_{0.47}As$
thickness	25 nm	100 nm	15 nm	100 nm
doping	$9\cdot10^{12}/cm^2$	$5\cdot10^{19}/cm^3$	$9\cdot10^{12}/cm^2$	$5\cdot10^{19}/cm^3$
sheet resistivity	540 Ω	32 Ω	269 Ω	15 Ω
access resistivity per contact	120.8 Ω–μm	55.6 Ω–μm	68.2 Ω–μm	12.7 Ω–μm
metal/regrowth contact resistivity	2.1 Ω–μm 0.2 Ω–μm^2	4.6 Ω–μm 1.5 Ω–μm^2	3.0 Ω–μm 0.4 Ω–μm^2	3.0 Ω–μm 0.8 Ω–μm^2